Otsuru, Kakigi et al.	Assessing A-delta fiber fun- ction with lidocaine using intra-epidermal electrical stimulaion.	Journal of Pain		In press	
柿木隆介	脳における痛みの認知	Brain Medical	21	211-216	2009
柿木隆介	痛みと脳機能	ペインクリニック	30	895-904	2009
柿木隆介	ヒトでの痛みの機序に関する研究－脳機能画像を中心に－	Clinical Neuroscience	27	514-517.	2009
武智詩子、魚住武則、辻貞俊	反復磁気刺激の治療への応用	臨床神経生理学	37	471-479	2009
下川敏雄、武藤由香里、御園生拓・北村眞一	アンサンブル学習法の河川景観満足度調査データ解析への応用	景観・デザイン論文集	6	41-50	2009
下川敏雄、後藤昌司	データ適応型分布に基づく多分岐型樹木構造接近法	計算機統計学	22	3-21	2009

In: Textbook of Therapeutic Cortical Stimulation
Editor: Sergio Canavero

ISBN 978-1-60692-537-9

Chapter 2

FROM LOCALIZATION TO SURGICAL IMPLANTATION

Youichi Saitoh* *and Koichi Hosomi*
Department of Neurosurgery, Osaka University Graduate School of Medicine, Japan.

ABSTRACT

In its landmark paper introducing MI ECS for the treatment of central pain, Tsubokawa et al (1991) included a brief description of the localization of the motor cortex:

"Location of the motor cortex was estimated by bony landmarks with conventional methods. Paramedian incision was made 1-4 cm lateral to the midline contralateral to the painful area. The trephination was then placed over the estimated area of the motor cortex. ... The locations of the sensory and motor cortices were confirmed from phase reversal of the N20 wave of somatosensory evoked potential recorded from the electrode. When the electrode was moved from the sensory cortex to the motor cortex, the N_{20} wave turned positive. The location of the motor cortex was again confirmed by motor evoked potential recoded in response to stimulation with the electrode. The motor cortex was mapped as carefully as possible and the electrode was placed in the region where muscle twitch of painful area could be observed at the lowest threshold".

Identification of the precise location of the central sulcus remains one of the key steps in this kind of surgery, and several techniques have been used for this purpose, although they have not been systematically compared. Most neurosurgeons use classical anatomical landmarks to determine the exact position for a craniotomy (chapter 1). Somatosensory evoked potentials (SSEP) and intraoperative motor evoked potential (MEP) measurements are also employed. In recent years, navigation systems have become increasingly important.

* Correspondence concerning this article should be addressed to: Dr. Youichi Saitoh, M.D., Ph.D. Department of Neurosurgery and Center for Pain Management, Osaka University Graduate School of Medicine, 2-2 Yamadaoka, Suita, Osaka 565-0871 Japan. Tel: +81-6-6879-3652; Fax: +81-6-6879-3659; e-mail: neurosaitoh@mbk.nifty.com; saitoh@nsurg.med.osaka-u.ac.jp.

There is no current consensus on the ideal surgical approach. Most neurosurgeons implant an electrode in the epidural space, but some implant it subdurally or in the interhemispheric or within the central sulci. The direction of the implanted paddle also remains controversial. This chapter summarizes and compares these various procedures.

ANATOMICAL LOCALIZATION

As detailed in chapter 1, there are several landmarks for detecting the location of central sulcus on the scalp and cortical surface. The central sulcus can be expected to lie approximately 4 - 5.4 cm posterior to the coronal suture on the scalp midline, and can be localized with the aid of Taylor-Haughton lines (Figure 1). The central sulcus is easily located with preoperative magnetic resonance imaging (MRI): it is characterized by the lack of sulcal branches, and lies just anterior to the pars marginalis of the cingulate sulcus on the interhemispheric surface (Naidich et al 1995, 2001). Oblique MRI views easily show the central sulcus (Figure 2). Penfield's Homunclus is commonly used for identification of the corresponding body parts on the precentral or postcentral gyrus. As discussed in chapter 1, the precentral knob sign corresponding to the hand is easily identified on surface MRI anatomic scans. From these findings, the position for the craniotomy can be decided.

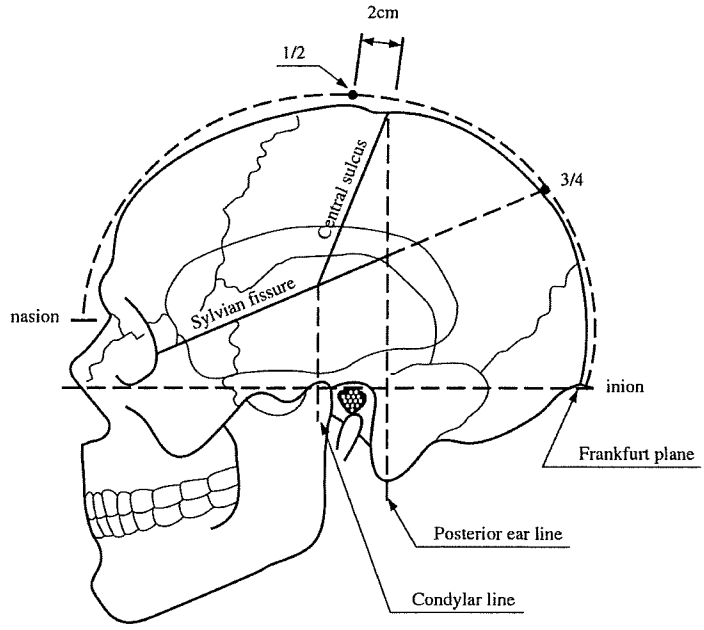

Figure 1. Taylor-Haughton line indicates the position of the central sulcus from the scalp.
Taylor-Haughton (T-H) lines can be constructed on an angiogram, CT scout film, or skull x-ray, and can then be reconstructed on the patient based on visible external landmarks. The Frankfurt plane (a.k.a. baseline) is the line from the inferior margin of the orbit through the upper margin of the external auditory meatus (EAM) (as distinguished from Reid's base line, running from the inferior orbital margin through the center of the EAM). The distance from the nasion to the inion is measured across the top of the calvaria and is divided into quarters (this can be done simply with a measuring tape). The posterior

ear line runs perpendicular to the baseline through the mastoid process (intersecting the skull sagittal midline about 1 cm behind the vertex and 3-4 cm behind the coronal suture). The condylar line runs perpendicular to the baseline through the mandibular condyle (intersecting the line representing the sylvian fissure). The Sylvian fissure (a.k.a. lateral fissure) is approximated by a line connecting the lateral canthus to the point 3/4 of the way posterior along the arc running over convexity from nasion to inion (or by a line drawn 45° to Reid's line starting at the pterion). A point 5 cm straight up from the external auditory meatus intercepts MI. The angular gyrus (which includes Wernicke's area) is located just above the pinna, with significant individual variability in its location.

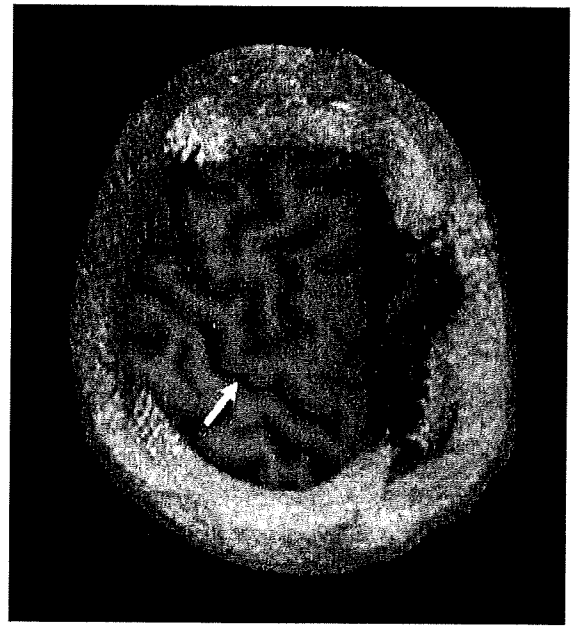

Figure 2. Reconstructed oblique MRI view of the central sulcus (arrow: central sulcus).

A simple way to locate the motor strip is to use a Callosal Grid system (Lehman and Kim 1995). Establishing a horizontal plane (HP) through the inferior border of the genu and the splenium of the corpus callosum creates such a proportional grid system. Three vertical planes perpendicular to HP are constructed: the anterior callosal plane (AC), the posterior callosal plane (PC), and the midcallosal plane (MC) in the midpoint between the AC and MC. If the grid is overlapped over the cortical surface, the junctional point between the HP and the MC corresponds with the inferior point of the central sulcus, where a central artery enters the central sulcus. The superior central sulcus lies 4mm anterior to PC. Imaginary lines connect the inferior and superior points that constitute the central sulcus.

ELECTROPHYSIOLOGICAL LOCALIZATION

SSEPs can be measured by stimulating the contralateral median nerve at the wrist; stimuli consist of single shocks (0.5 ms, 4.7 Hz, 20 mA) to produce a small, but consistent contraction of the thumb. SSEPs are recorded from each cortical electrode referenced to the ipsilateral ear

lobe. Individual SSEP signals are differentially amplified and filtered: 200 are averaged through a digital signal analyzer with sample interval of 40 mcsec. The phase reversal of the N20 (sensory cortex) /P20 (motor cortex) waves is used to confirm the location of the central sulcus (Wood et al 1988, Velasco et al 2002), using a 20/32-contact grid and the central scalp EEG leads or directly using the definitive 4-contact strip overlying the dura (Figure 3). Polarity inversion of potentials across the sulcus is less reliable and technically more difficult for trigeminal SEPs (McCarthy et al 1993) and only occasionally a phase reversal has been described for tibial nerve SEPs (Maegaki et al 2000). Other later components (P25-N25; P30-N30) also present phase reversals, but may not be observed. Phase reversal seems to be a rather constant feature of SSEPs, provided that the orientation of the electrode is perpendicular to the Rolandic fissure, otherwise it may not be present. The Rolandic fissure being tortuous and oblique along the convexity of the brain, it is difficult to believe that phase reversal may be obtained in all cases without the assistance of visual inspection of the sulci, as in the case of epidural recordings (Velasco et al 2002). Although N20 is generally recordable, the P20 component may be missing, even in awake or mildly sedated patients, in part due to the dipole generator of the early component at each side of the fissure which, having an oblique depth posterior trajectory with respect to the cortical surface, orients the N20 component toward the surface and the P20 component toward the depth. Moreover, the N20/P20 reversal is only useful for hand representation targeting. The rolandic tortuosity that in some parts becomes parallel to the midsagittal line complicates the placement of the 4-contact strip on MI by determining reversal only in a single point. Even worse, maximal N20 amplitude can be reached on either motor or sensory cortex in several patients (Wood et al 1988, Velasco et al 2002). Both components can be severely attenuated by nervous system lesions: patients with phantom-limb pain, brachial plexus avulsion, severe stroke or other similar conditions may thus show no SSEPs.

Most importantly, inferring the position of the motor hand area from the position of the maximum amplitude median nerve SEP is impossible. Indeed, Woolsey et al (1979) demonstrated that the face-arm boundary is situated more laterally on the postcentral gyrus than on the precentral gyrus, by 1–2 cm. It is therefore necessary to map the motor cortex. Penfield and Boldrey (1937) first systematically stimulated the sensory-motor cortex and described the sensory and motor "homunculus". They utilized a bipolar direct stimulation of the cortex, applying 50–60 Hz stimuli up to 20 mA for 1–4 s, and looked for movements or sensations in the awake patient. This technique required awake surgery, often induced complex movements involving more than one muscle and provoked epileptic seizures in a high percentage of cases (20–25%). As regards the leg representation, Woolsey et al (1979) found that in only one third of the cases the lower extremity is on the medial surface of the hemisphere, in two thirds of the cases it extends on the lateral surface and, in 27% of the cases, the whole lower extremity is on the lateral surface. Recently, an enlarged and displaced motor map for the hand area was described in Parkinson's disease patients. Map shifts were found in the majority of the patients (12/15), both in untreated early cases and treated cases of long duration, with a correlation between the inter-side difference in the severity of PD symptoms (UPDRS) and interhemispheric map displacement (Thickbroom et al 2006). In sum, guidance of epidural electrode placement is often inadequate or impossible by SSEPs.

According to Velasco et al (2002), recording corticocortical evoked responses (CCER) is simple and reliable and superior to SSEPs. MI stimulation elicits negative CCER over the frontal scalp, whereas SI stimulation elicits positive responses over parietal and occipital scalp regions.

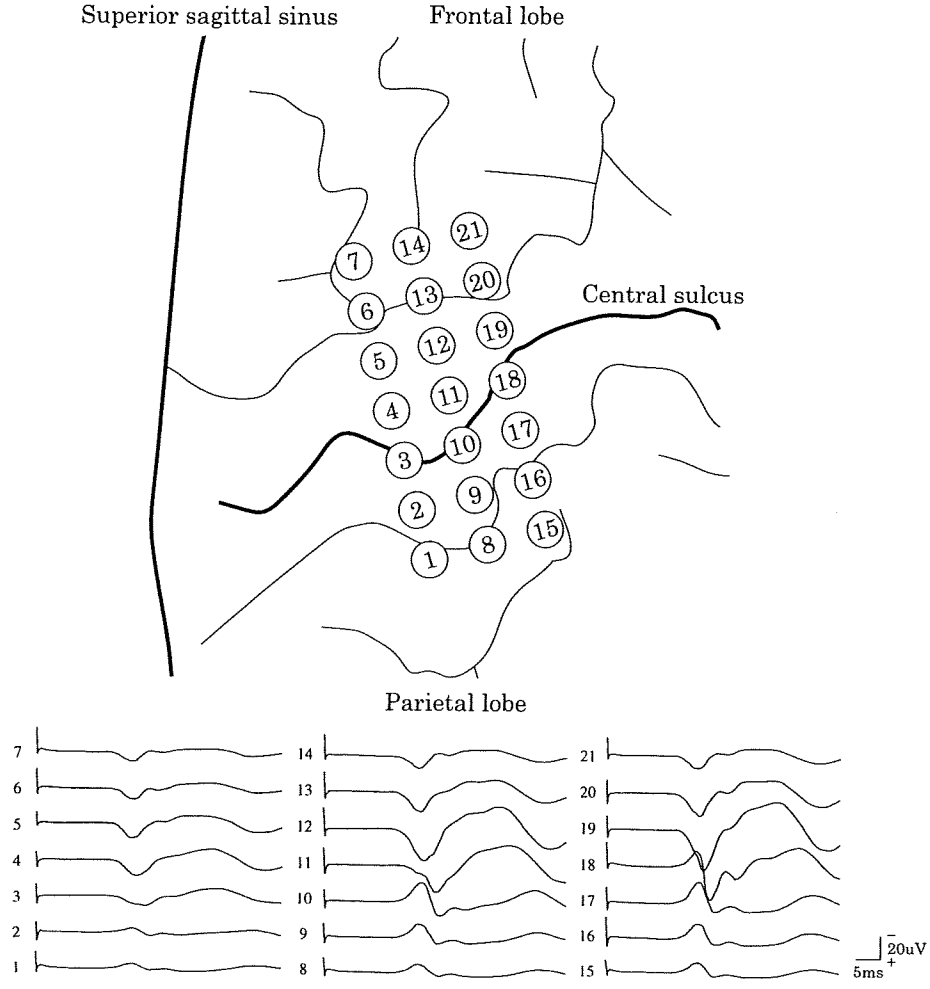

Figure 3. SSEPs show phase reversal of the N20 wave, when the median nerve is stimulated. The black wide line indicates the estimated location of the central sulcus.

Most neurosurgeons attempt intraoperative test stimulation by using the quadripolar or the grid electrodes. Test bipolar stimulation (210-1000 μs –generally 400-500-μs, 1-5 Hz up to 100Hz, at increasing voltage or intensity –up to 50 mA, anodally, but also cathodally) is applied by means of the contacts situated over the motor or sensory cortex. In general, the amplitude needed to produce motor responses is higher using epidural rather than subdural stimulation. Motor contraction can be elicited at relatively lower amplitudes when general anesthesia is not employed. 1Hz stimulation is preferred to higher frequencies, since the former does not habituate and has less potential to trigger seizures. Muscle responses are recorded

from muscle bellies of the contralateral hemibody, with EMG needle electrodes or visually. The supposed advantage of a grid electrode is nixed by the observation that over 75% of the cortical surface is not covered by its contacts, not to mention the imperfect superposition with the definitive strip electrode.

Under local anesthesia, the patients may describe pain reduction, paresthesias in the painful body part, muscle twitching or contraction or nothing at all (Canavero and Bonicalzi 2002, Velasco et al 2002). Interestingly, stimulation of both MI and SI can elicit similar motor or sensory responses and both motor and sensory responses can be obtained from the same contacts (Schmid et al 1980, Wood et al 1988, Canavero and Bonicalzi 2002, 2007), making it difficult to rely on motor and sensory responses to differentiate MI from SI.

In some institutions, motor evoked potentials (MEPs) are measured under general anesthesia. Holsheimer et al (2007) stressed the importance of intra-operative MEP measurement obtained by monopolar and bipolar stimulation for determining the location of the electrodes bringing most pain relief during chronic ECS. Monopolar stimulation appeared superior at determining the optimal point for chronic motor cortex stimulation. They concluded that the anode yielding the largest intra-operative MEP should be selected as the cathode for chronic stimulation. Intraoperative D-wave recording of corticospinal MEPs have been utilized to optimize electrode placement; the D-wave has been recorded with a flexible wire electrode placed epidurally in the cervical (C3-4) spinal cord during high intensity anodal monopolar stimulation of each plate electrode under general anesthesia. The aim was to evoke the D-wave of highest amplitude. Pain reductions significantly correlated with the recorded amplitude of the D wave employing the same stimulation electrode. The result was analgesia with lower voltages than generally required (Yamamoto et al 2007).

LOCALIZATION BY FUNCTIONAL MRI (FMRI)

fMRI has been explored extensively in terms of functional localization. In particular, sequential tapping of fingers in a predetermined fixed order or repetitive opposition of the thumb and each of the remaining fingers activates MI contralaterally (but also the ipsilateral MI, supplementary motor and premotor areas and the primary somatosensory areas bilaterally). This method appears to be superior to the competing methods described above. Pirotte et al (2005) utilized fMRI to identify the hand and tongue motor area. fMRI data were coregistered on 3D T1-weighted MRI anatomical scans and matched with data from intraoperative neurophysiology. The operation was performed under TIVA (see ahead); they utilized median-nerve SEP phase reversal to identify the central sulcus and mapped the motor cortex using the 60 Hz Penfield's technique. In 61% of cases, they found a good correlation between fMRI and intraoperative neurophysiological data, with a mean distance of 3.8 ± 1.3 mm between the two hot spots, which is sufficiently accurate, considering that the activation area of an electrode measures 5 mm; in 33% of the cases, intraoperative neurophysiology provided ambiguous results because of electrical artifacts, influence of anesthesia, SEP attenuation, diffuse motor responses, or sensorimotor disconnection. Some of these problems were due to an inadequate mapping technique; in 6% of the cases they reported poorly localization with both fMRI and intraoperative neurophysiology.

Blood oxygenation level depending (BOLD) fMRI data of motor functions of the tongue, arm or leg are obtained by using standardized paradigms, such as repetitive contraction of the lips, cyclic finger tapping of the contralateral hand, or flexion-and-extension of the toes of the contralateral foot at a rate of 1 Hz after a training session before imaging is performed. Post-stroke motor deficits may hamper examination, but fMRI is particularly useful for amputees or plexus avulsion patients, since virtual movements of the phantom or paralytic limb easily induce contralateral precentral and postcentral gyri activations. Blocks of 30 seconds of alternating activation and rest are repeated a few times (Canavero and Bonicalzi 2007). Generally, a focal cortical activation area (diameter 5-10 mm) after hand motor tasks is localized to the contralateral precentral gyrus, but differences between the two sides in the surface and minor displacements of the precentral activation area are frequently observed (also due to cortical remapping). It remains a matter of debate which area is more suitable as a stimulation target, the mirror image of the activation site on the healthy side or the displaced activation site on the affected side. Stippich et al (2004) developed a fully automated super-fast fMRI method for SI localization.

Diffusion tensor imaging (DTI) tractography has been suggested as a means to identify the motor cortex (Kamada et al 2005), but it should be taken in mind that TDI is a mathematical probability function, not an anatomical image.

Central sulcus veins have been used as landmarks during subdural approaches, but, being sometimes located deep in the sulcus, cannot be identified by examining only the cortical surface (Saitoh and Yoshimine 2007).

NEURONAVIGATION

Several kinds of navigation systems for neurosurgical assistance can be used to estimate the position of the central sulcus or other structures, both on the dura mater and scalp (Tirakotai et al 2007). Neuronavigation combined with fMRI data help to decide the best position for craniotomy and for placement of the stimulating paddle (Rasche et al 2006). While in most cases fMRI data can be satisfactory matched with navigation data, in some cases, motion artifacts and low signal levels interfere with fMRI data analysis. A drawback of neuronavigation is the requirement that the patient's head be fixed in a 3-point pin holder or vacuum headrest (Tirakotai et al 2007), which several patients may not tolerate under local anesthesia. For this reason, other surgeons prefer not to fix the patient's head and operate without navigation.

TECHNIQUES OF IMPLANTATION

Implanted electrodes used in reported studies have generally been Resume (Medtronic) or Lamitrode (ANS) stimulating quadripolar strips; eight-contact paddles have been used in one failed trial (NCT00122915). Most neurosurgeons (including Tsubokawa) implant the strip in the epidural space, but a few insert the strip subdurally (Saitoh et al 2000, 2007, Kleiner-

Fisman et al 2003, Strafella et al 2007). In patients with extensive painful areas, two strips are positioned.

Anethesia is induced with a loading dose of Remifentanil 3–4 ng/ml in continuous infusion followed after 5–8 min by Propofol 5.5 μg/ml as induction dose (Total intravenous anesthesia, TIVA). Endotracheal intubation is facilitated by vecuronium bromide 0.1 mg/kg; no further doses of muscle relaxants are administered throughout surgery. The lungs are mechanically ventilated with a 50% O2 in air mixture, in order to maintain end tidal concentrations of CO2 (ETCO2) at 30–35 mmHg. Anesthesia is maintained with Remifentanil (5–6 ng/ml, up to 7-8 ng/ml if necessary) and Propofol (2.5-3.0 μg/ml). At the end of the surgical procedure, all patients are awakened within 15–30 min from cessation of TIVA.

A small craniotomy or burr-hole is made around the central sulcus. The four-contact electrode array (each contact 5 mm in diameter; inter-contact distance center-to-center 1 cm) is usually placed in the epidural space. The best location and orientation of the electrode array are generally determined in such a way that bipolar stimulation with an appropriate pair of electrodes can be attained. Some surgeons place the electrode perpendicular to the central sulcus above the precentral (cathode) and postcentral (anode) gyri for the supposed improved selectivity (e.g. Nguyen et al 1999), others in a parallel fashion, i.e. with all contacts on MI or SI (e.g. Canavero and Bonicalzi 2002, Rasche et al 2006), but there appears to be no difference between the results of these two approaches (Tsubokawa et al 1991, 1993). Moreover, no polarity-related difference in pain relief is seen for most patients with epidural electrodes (Katayama et al 1998).

Saitoh et al (2000; Hosomi et al 2008) implanted the paddle subdurally on the cerebral or interhemispheric surface) or within the central sulcus. The latter makes it possible to stimulate the primary motor cortex more directly (Takahashi et al 2002, White et al 1997). Nuti et al (2005) implanted the strip electrode on the interhemispheric surface to treat leg pain. In some patients with brain atrophy, the cortical surface and the dura mater are wide apart, in which case patients may fail to respond to extradural stimulation: a subdural approach may be considered in a few, highly select cases.

After the implantation of the electrodes, a test period of a few days to 2-4 weeks follows. If the stimulation proves effective, under general anesthesia, a pulse generator is then implanted subcutaneously below the clavicle and connected to the paddle via a subcutaneous extension. For movement disorders patients, a single surgical procedure may be used (Canavero and Bonicalzi 2007b).

Stimulating paddles have been implanted through several approaches:

1-Epidural Single Burr-Hole (Figure 4)

Both Tsubokawa et al (1991) and Meyerson et al (1993) performed MI ECS using a single burr-hole made on the central sulcus under local anesthesia. For leg pain, a paddle is placed on the medial edge of the hemisphere, but involves some risk of developing an epidural hematoma. This technique may require relocations before an optimal position is found, and thus increase the risk of epidural bleeding due to dural detachment. However, this was not a problem in recent navigated series (Rasche et al 2006).

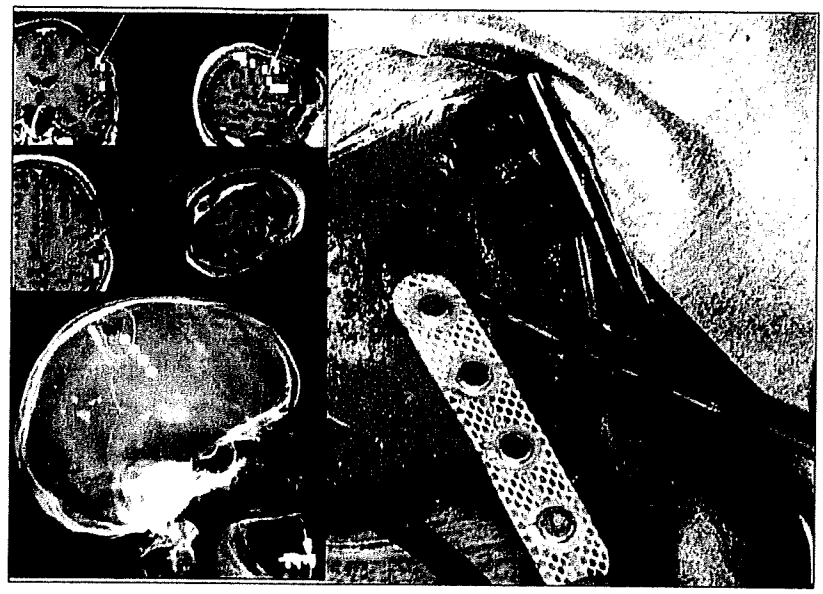

Figure 4. Single burr-hole surgery with the assistance of neuronavigation system and fMRI (courtesy of Dr. Rasche). Insertion of the stimulating paddle (which is shown reversed for clarity) is performed via a single burr hole.

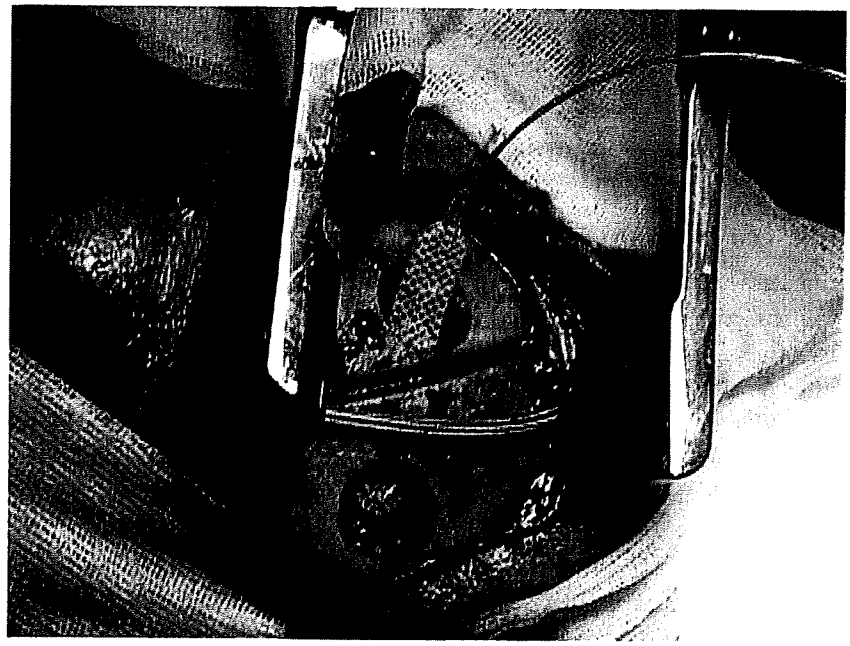

Figure 5. Two burr-hole surgery is shown. The locations of burr holes are marked on the scalp depending on the anatomical landmarks (courtesy of Prof. Canavero).

2-Two Epidural Burr-Holes (Figure 5)

Canavero (Canavero and Bonicalzi 2002) makes an oblique linear skin incision (6-10cm) parallel to and 1 cm ahead of or behind the projection of the central sulcus and then drills two burr holes at a distance of 2-4 cm (plus a bony groove parallel to the paddle to accommodate the connector between the looping lead and the extension). A stimulating paddle is inserted from the edge of one burr hole into the epidural space overlying the precentral gyrus or post central gyrus contralateral to the painful area or most disabled side for movement disorders. The bony bridge between the two holes will then hold the plate in place and simultaneously reduce the durocortical gap. For facial or leg targets, the paddle can be gently advanced caudally or rostrally by up to 2 cm. This technique entails no risk of epidural hematoma, and accidental displacement of the electrode has never been observed (S Canavero, personal communication).

3-Epidural Bone flap

Because of greater availability of the epidural area for electrophysiological exploration and mapping, the procedure has been proposed to result in improved outcome (Nguyen et al 1999), but this has not been confirmed. A small craniotomy (4-5 cm) is made on the central sulcus. The center of the craniotomy should correspond to the target as determined by imaging. This technique allows SSEP recordings from electrodes placed on the dura mater. The paddle is fixed to the dura mater with two stitches (making accidental displacement impossible), which may theoretically catch on a vessel and cause intracerebral bleeding. The risk of inadvertent opening of the dura during bone detachment must be borne in mind.

4-Subdural Method

In patients with advanced cortical atrophy, epidural stimulation may fail due to the duro-cortical separation. The cortical surface and interhemispheric surfaces subdurally may be elected as targets for stimulation. However, large bridging veins sometimes interfere with implantation on the interhemispheric surface and adhesion may occur due to subarachnoid hemorrhage. Moreover, dissection of the central sulcus involves the risk of developing new neurological deficits due to brain damage or vein obstruction. For upper limb and/or face pain, the arachnoid membrane of the central sulcus must be carefully dissected and the vessels within the central sulcus must be freed with a microsurgical procedure to expose the hidden lateral walls of the precentral and postcentral gyri (Saitoh et al 2006). Since the paddle is too stiff to be placed within the central sulcus, it must be trimmed off (Figure 6). Saitoh et al (2000) limited most of the implantations within the central sulcus to patients with severe motor weakness or lack of function. In their series, test stimulation of MI within the central sulcus was more effective in most cases than was subdural stimulation on the cerebral surface, but long-term clinical results were not on a par with ECS (Saitoh and Yoshimine 2007) and patients who received the implantation within the central sulcus gained only temporary pain

reduction (maximum: 6 months) (Hosomi et al 2008). At the end of surgery, the lead extension is fixed to the dura or the border of the burr hole with a silk suture to prevent dislocation. However, migration of the electrodes seems to be more of a problem with a subdural than an extradural approach. A meticulous, watertight dural closure is mandatory to minimize the risk of cerebrospinal fluid leakage.

Figure 6. After trimming to reduce stiffness, a Resume paddle is implanted within the central sulcus.

COMPLICATIONS

Of all published cases of invasive cortical stimulation, 11.4% were associated with one or more adverse effects. Speech disorders (aphasia/dysarthria), although rare and generally temporary, have been observed (Ebel et al 1996, Canavero and Bonicalzi 2002). Some cases of headache reportedly associated with stimulation of the face area may actually be due to contraction of the temporalis muscle (Canavero and Bonicalzi 2002). However, local pain may be relieved by incision and resuturing of the dura around the electrode or, more simply, by bipolar coagulation. Other reported side effects include fatigue, paresthesia and dysesthesia (2.2% of cases), but also, exceptionally, impairment in motor imagery tasks (Tomasino et al 2005) and supernumerary phantom arms (Canavero and Bonicalzi 2002, 2007).

Montes et al (2002) analyzed event-related potentials (ERPs) and behavioral performance during an auditory target-detection task in 11 consecutive patients obtained during MI ECS and 10 minutes after switching off stimulation. While sensory responses remained unaffected by MCS, there was a significant delay of brain potentials reflecting target detection in the older patients (N2 and P3), rapidly reversible after MI ECS discontinuation. No effect was observed in patients younger than 50 years. Individually, the effect was highly variable from no effect to

a delay of tens of milliseconds. Cognitive effects of MCS appeared as mild and non-specific, directly related to the stimulation period (i.e. with no post-effect), in a manner reminding of cognitive effects reported during MI rTMS. Thus, MCS may interfere with relatively simple cognitive processes such as those underlying target detection, notably in the elderly and in the presence of preexistent cerebral lesions.

Occurrence of epileptic seizures, probably due to differences in testing conditions, has been reported during test stimulation in a minority of patients. The low rate of epileptic seizures during chronic stimulation (0.2%) means that stimulation of MI within an appropriate range of parameters is reasonably safe. The most serious reported complications are epidural or subdural hematomas. These are definitely exceptional with an extradural approach, and some surgeons never observed one, making the risk of peri-operative hemorrhage much lower compared to deep brain stimulation. However, in our series using a subdural approach, two patients developed cerebral hemorrhage: one died and the other remained in a vegetative state (Hosomi et al 2008). This is especially true for patients with post-stroke pain, who are likely to develop a new stroke in the years following the first one.

Some wound infections have been reported by most surgeons. If the infection occurs, all devices including the paddle, extension leads, and pulse generators must be removed temporally. Patients with post-stroke pain frequently have diabetes mellitus and thus are at greater risk.

The implanted pulse generator (IPG) can accidentally turn off due to electromagnetic interference from household devices in close (<10 cm) proximity, such as electric appliances of any kind, but also anti-theft devices and metal detectors or magnets in loudspeakers.

At impedances >2000 Ω, a connection problem, such as a broken cable or a lead fracture, must be suspected. The operator should thus measure impedance in a unipolar configuration in order to assign a value to the single contact. The so-called radio test may be useful: IPGs emit a signal at 500-550 kHz which can be received as a continuous hum on a small battery operated AM radio receiver.

SAFETY OF STIMULATORS

The output of commercial stimulators are either of the "controlled current" (CC) or "controlled voltage" (CV) type. CC output circuits are somewhat more complex and less power-efficient than the CV type, but may provide a more stable level of stimulation, especially where the electrode impedance may fluctuate as a result of e.g. changing contact with tissue, formation of scar tissue, polarization potentials on the metal/electrolyte interface. Most of the stimulus voltage of macro-electrodes is dissipated in the impedance of the tissue. If the impedance changes in a CC circuit, the output voltage automatically rises to keep the current flow constant. If the impedance changes in a CV circuit, the voltage stays the same and the current changes.

Stimulators use pulsatile rather than sinusoidal current waveforms. The stimulus waveform may be monophasic or biphasic. In biphasic stimulation, the negative voltage applied is balanced by an equal amount of positive voltage. This is generally considered to be far safer than monophasic stimulation as it allows for a balance of ionic exchange at the electrode-cortex interface. If the charge is not balanced, it is possible that metal ion deposition will occur at the

interface, which may cause deleterious effects for both the tissue and the electrode (Polikov et al 2005). A fast-rising rectangular pulse of negative current is the most efficient stimulating waveform.

Each pulse delivers a charge (Q) of current per phase (CPP):

(1) $Q = A \times PW$

Charge density (CD) of the different cathodal pulses is given by:

(2) $QD = A \times PW / cathodal\ area.$

These formulae indicate that:

1) maximal safety (i.e. minimal tissue damage) is obtained by applying short pulse durations (Crago et al 1974), i.e. slightly greater than chronaxie, which are also ideal to evoke neuronal responses (Tehovnik 1996).
2) QD for a given current is limited by the size of the electrode: more current is required to stimulate the cortex using large electrode than using small electrodes, but decreasing the surface area of the electrode may increase the extent of histological damage. Consequently, paddle or strip electrodes containing multiple contacts are ideal to recruit more neurons in the stimulation field. The QD threshold is lower when using surface electrodes (ECS) versus depth electrodes (DBS). Luckily, functional alteration can be achieved by charge densities much lower than those required for histological damage.

The least damaging pulse waveform is that with no net direct current (DC), which can lead to tissue damage even at very low intensity. The current density and charge per phase (CPP)- but not frequency, waveform or periods between pulses- are likely the most important factors in determining safety of a particular stimulation protocol (McCreery et al 1990). Ideally, the CPP and current density ought to be minimized. According to Pudenz et al (1975, 1977), CPP must not exceed 0.3 μC(oulombs) in each half of the stimulating pulse. In a human study, subdural stimulation with 0.3 ms square wave pulses at 50 Hz and 12.5-15 mA delivered for 24 hours achieved a maximum CPP of 4-4.4 μC, with a maximum charge density of 52-57 μC/cm2, which suggests a greater ability of the human brain to accommodate higher currents and current densities (Gordon et al 1990). Choice of stimulation features must aim to prevent electrode dissolution and generation of electrochemical toxic products at the electrode interface (by electrode polarization and hydrolysis: Bartlett et al 1977). Electrodes should be made of corrosion-resistant noble metals or alloys, such as platinum-iridium (actually, there is a small corrosion rate, which may in principle lead to toxic cumulative effects over many years). *A charge-balanced symmetrical biphasic waveform with two closely spaced pulses of equal charge, cathodal followed by anodal, is the stimulus waveform recommended for avoiding tissue damage and electrode corrosion.* In fact, the electrochemical reactions occurring during the first pulse (phase) are reversed by the following pulse of opposite polarity. However, biphasic symmetrical stimulus waveforms result in less selectivity than monophasic waveforms.

Prolonged stimulation at an intensity well below threshold for histologically detectable neural damage may nonetheless induce pronounced and prolonged elevation of the electrical threshold of stimulated neurons.

REFERENCES

Bartlett JR, Doty RW, Lee BB, Negrao N, Overman WH, Jr. Deleterious effects of prolonged electrical excitation of striate cortex in macaques. *Brain Behav Evol* 1977;14:46-66.

Canavero S, Bonicalzi V: Therapeutic extradural cortical stimulation for central and neuropathic pain: A review. *Clin J Pain* 18:48-55, 2002

Canavero S, Bonicalzi V: Extradural cortical stimulation for central pain. In: D Sakas, B Simpson, E Krames, eds. *Operative Neuromodulation*. Vol.2. Wien: Springer-Verlag, 2007, pp 27-36

Canavero S, Bonincalzi V. Extradural cortical stimulation for movement disorders. In: D Sakas, B Simpson, E Krames, eds. *Operative Neuromodulation*. Vol.2. Wien: Springer-Verlag, 2007b, pp 223-232

Crago PE, Peckham PH, Mortimer JT, Van der Meulen JP. The choice of pulse duration for chronic electrical stimulation via surface, nerve, and intramuscular electrodes. *Ann Biomed Eng* 1974;2:252-264.

Ebel H, Rust D, Tronnier V, Spies EH, Boker D, Kunze S: Chronic precentral stimulation in trigeminal neuropathic pain. *Acta Neurochir* 1996; 138:1300-6.

Gordon B, Lesser RP, Rance NE, et al. Parameters for direct cortical electrical stimulation in the human: histopathologic confirmation. *EEG Clin Neurophysiol* 1990; 75: 371-377

Holsheimer J, Lefaucheur JP, Buitenweg JR, Goujon C, Nineb A, Nguyen JP. The role of intra-operative motor evoked potentials in the optimization of chronic cortical stimulation for the treatment of neuropathic pain. *Clin Neurophysiol* 2007; 118: 2287-2296

Hosomi K, Saitoh Y, Kishima H, Oshino S, Hirata M, Tani N, Shimokawa T, Yoshimine T: Electrical stimulation of primary motor cortex within the central sulcus for intractable neuropathic pain. *Clin Neurophysiol* 2008; 119: 993-1001

Kamada K., Sawamura Y., Takeuchi F., et al. Functional identification of the primary motor area by corticospinal tractography, *Neurosurgery Suppl.1* 2005; 56: 98—109

Katayama Y, Fukaya C, Yamamoto T. Poststroke pain control by chronic motor cortex stimulation: neurological characteristics predicting a favorable response. *J Neurosurg* 1998;89:585-91.

Kleiner-Fisman G, Fisman DN, Kahn FI, Sime E, Lozano A, Lang AE. Motor cortical stimulation for Parkinsonism in Multiple Systemic Atrophy *Arch Neurol* 2003; 60:1554-1558

Lehman RM, Kim HI. Partial seizures with onset in central area: Use of the callosal grid system for localization. *Acta Neurochir* 1995;64:79-82.

McCarthy G., Allison T., Spencer D.D. Localization of the face area of human sensorimotor cortex by intracranial recording of somatosensory evoked potentials, *J Neurosurg* 1993; 6:874—884

McCreery DB, Agnew WF, Yuen TG, Bullara L. Charge density and charge per phase as cofactors in neural injury induced by electrical stimulation. *IEEE Trans Biomed Eng* 1990; 37, 996-1001

Maegaki Y., Najm I., Terada K., et al. Somatosensory evoked high-frequency oscillations recorded directly from the human cerebral cortex. *Clin Neurophysiol* 2000; 111:1916—1926

Meyerson BA, Lindblom U, Linderoth B, Lind G, Herregodts P. Motor cortex stimulation as treatment of trigeminal neuropathic pain. *Acta Neurochir* 1993; 58:150-153.

Montes C, Mertens P, Convers P, et al. Cognitive effects of precentral cortical stimulation for pain control: an ERP study. *Clinical Neurophysiology* 2002;32: 313-325

Naidich TP, Valvanis AG, Kubik S: Anatomical relationships along the low-middle convexity: part 1: normal specimens and magnetic resonance imaging. *Neurosurgery* 1995; 36: 517-532

Naidich TP, Blum JT, Firestone MI. The parasagittal line: an anatomic landmark for axial imaging. *AJNR* 2001; 22:885-895

Nguyen JP, Lefaucheur JP, Decq P, et al. Chronic motor cortex stimulation in the treatment of central and neuropathic pain. Correlations between clinical, electrophysiological and anatomical data. *Pain* 1999;82:245-51.

Nuti C, Peyron R, Garcia-Larrea L, Brunon J, Laurent B, Sindou M, Mertens P: Motor cortex stimulation for refractory neuropathic pain: Four year outcome and predictors of efficacy. *Pain* 2005; 118: 43-52.

Penfield W , Boldrey E. Somatic motor and sensory representation in the cerebral cortex of man as studied by electrical stimulation *Brain* 1937; 60:389-443

Pirotte B, Neugroschl C, Metens T, et al. Comparison of Functional MRI-Guidance to Electrical Cortical Mapping for Targeting Selective Motor Cortex Areas in Neuropathic Pain: A Study Based on Intraoperative Stereotactic Navigation. *AJNR Am. J. Neuroradiol.* 2005; 26:2256-2266.

Polikov VS, Tresco PA, Reichert WM. Response of brain tissue to chronically implanted neural electrodes. *J Neurosci Methods* 2005; 148, 1-18.

Pudenz RH, Bullara LA, Jacques S, Hambrecht FT. Electrical stimulation of the brain. III. The neural damage model. *Surg Neurol* 1975; 4: 389-400

Pudenz RH, Agnew WF, Bullara LA. Effects of electrical stimulation of brain. *Brain Behav Evol* 1977; 14: 103-125

Rasche D, Ruppolt M, Strippich C, Unterberg A, Tronnier VM. Motor cortex stimulation for long-term relief of chronic neuropathic pain: A 10 year experience. *Pain* 2006; 121: 43-52

Saitoh Y, Shibata M, Hirano S, Hirata M, Mashimo T, Yoshimine T: Motor cortex stimulation for the central and the peripheral deafferentation pain. *J Neurosurg* 2000; 92:150-155

Saitoh Y, Yoshimine T. Stimulation of primary motor cortex for intractable deafferentation pain. In: D Sakas, B Simpson, E Krames, eds. *Operative Neuromodulation*. Vol.2 Wien: Springer-Verlag, 2007, pp. 51-6.

Schmid D, Ebeling U, reulen HJ. Electrophysiological localization of the human sensorimotor cortex. *J Neurosurg* 1980; 70; 817-818

Stippich C, Romanovsky A, Nennig E, Kress B, Haehnel S, Sartor K. Fully automated localization of the human primary somatosensory cortex in one minute by functional magnetic resonance imaging. *Neurosci Lett* 2004; 364: 90-93

Strafella AP, Lozano AM, Lang AE, Ko JH, Poon Y-Y, Moro E. Subdural motor cortex stimulation in Parkinson's disease does not modify movement-related rCBF pattern. *Mov Disorders* 2007; 22: 2113-2116.

Takahashi N, Kawamura M, Araki S: Isolation hand palsy due to cortical infarction: localization of the motor hand area. *Neurology* 2002; 58:1412-4.

Tehovnik EJ. Electrical stimulation of neural tissue to evoke behavioral responses. *J Neurosci Methods* 1996;65:1-17.

Thickbroom GW, Byrnes ML, Walters S, Stell R, Mastaglia FL. Motor cortex reorganisation in Parkinson's disease. *J Clin Neurosci* 2006; 13: 639-42

Tirakotai W, Hellwig D, Bertalanffy H, Riegel T: Localization of precentral gyrus in image-guided surgery for motor cortex stimulation. In: D Sakas, B Simpson, E Krames, eds. *Operative Neuromodulation*. Vol.2 Wien: Springer-Verlag, 2007, pp. 75-79

Tomasino B, Budai R, Mondani M, Skrap M, Rumiati RI. Mental rotation in a patient with an implanted electrode grid in the motor cortex. *Neuroreport* 2005; 16: 1795-1800

Tsubokawa T, Katayama Y, Yamamoto T, Hirayama T, Koyama S. Chronic motor cortex stimulation of the treatment of central pain. *Acta Neurochir Suppl (Wien)* 1991;52:137-139.

Tsubokawa T, Katayama Y, Yamamoto T, Hirayama T, Koyama S. Chronic motor cortex stimulation in patients with thalamic pain. *J Neurosurg* 1993;78:393-401.

Velasco M, Velasco F, BritoF, Velasco AL, Nguyen JP, Marquez I, Boleaga B, Keravel Y: Motor cortex stimulation in the treatment of deafferentation pain. 1. Localization of the motor cortex. *Stereotact Funct Neurosurg* 2002;79:146-167.

Yamamoto T, Katayama Y, Obuchi T, et al. Recording of corticospinal evoked potentials for optimum placement of motor cortex stimulation electrodes in the treatment of post-stroke pain. *Neurol Med Chir (Tokyo)* 2007;47:409-414.

White LE, Andrewa TJ, Hulette C, Richards A, Groelle M, Paydarfar J, et al: Structure of the human sensorimotor system: I. Morphology and cytoarchitecture of the central sulcus. *Cereb Cortex* 1997;7:18-30

Wood CC, Spencer DD, Allison T, McCarthy G, Williamson PD, Goff WR: Localization of human sensorimotor cortex during surgery by cortical surface recording of somatosensory evoked potentials. *J Neurosurg* 1988; 68: 99-111.

Woolsey CN, Erickson T, Gilson WE. Localization in somatic sensory and motor areas of human cerebral cortex as determined by direct recording of evoked potentials and electrical stimulation. *J Neurosurg* 1979; 51:476-506.

NeuroImage 49 (2010) 2564–2569

Contents lists available at ScienceDirect

NeuroImage

journal homepage: www.elsevier.com/locate/ynimg

Modulation of neuronal activity after spinal cord stimulation for neuropathic pain; $H_2{}^{15}O$ PET study

Haruhiko Kishima [a], Youichi Saitoh [a,*], Satoru Oshino [a], Koichi Hosomi [a], Mohamed Ali [a], Tomoyuki Maruo [a], Masayuki Hirata [a], Tetsu Goto [a], Takufumi Yanagisawa [a], Masahiko Sumitani [d], Yasuhiro Osaki [b], Jun Hatazawa [c], Toshiki Yoshimine [a]

[a] Department of Neurosurgery, Osaka University, Graduated school of Medicine, Suita, Osaka, Japan
[b] Otorhinolaryngology, Osaka University, Graduated school of Medicine, Suita, Osaka, Japan
[c] Nuclear Medicine and Tracer Kinetics, Osaka University, Graduated school of Medicine, Suita, Osaka, Japan
[d] Department of Anesthesiology and Pain Relief Center, The University of Tokyo Hospital, Tokyo, Japan

ARTICLE INFO

Article history:
Received 8 July 2009
Revised 27 September 2009
Accepted 19 October 2009
Available online 27 October 2009

Keywords:
Neuropathic pain
Spinal cord stimulation
Regional cerebral blood flow

ABSTRACT

Spinal cord stimulation (SCS) is an effective therapy for chronic neuropathic pain. However, the detailed mechanisms underlying its effects are not well understood. Positron emission tomography (PET) with $H_2{}^{15}O$ was applied to clarify these mechanisms. Nine patients with intractable neuropathic pain in the lower limbs were included in the study. All patients underwent SCS therapy for intractable pain, which was due to failed back surgery syndrome in three patients, complex regional pain syndrome in two, cerebral hemorrhage in two, spinal infarction in one, and spinal cord injury in one. Regional cerebral blood flow (rCBF) was measured by $H_2{}^{15}O$ PET before and after SCS. The images were analyzed with statistical parametric mapping software (SPM2). SCS reduced pain; visual analog scale values for pain decreased from 76.1 ± 25.2 before SCS to 40.6 ± 4.5 after SCS (mean $\pm$ SE). Significant rCBF increases were identified after SCS in the thalamus contralateral to the painful limb and in the bilateral parietal association area. The anterior cingulate cortex (ACC) and prefrontal areas were also activated after SCS. These results suggest that SCS modulates supraspinal neuronal activities. The contralateral thalamus and parietal association area would regulate the pain threshold. The ACC and prefrontal areas would control the emotional aspects of intractable pain, resulting in the reduction of neuropathic pain after SCS.

Introduction

Neuropathic pain arises as a direct consequence of a lesion or disease affecting the somatosensory system (Loeser and Treede, 2008). It is generally more severe and more likely to be drug-resistant and persistent than nociceptive pain (Finnerup et al., 2005; Dworkin et al., 2003). Thus, chronic pain is often under-diagnosed and under-treated (Taylor, 2006), and it impairs quality of life. The causes of neuropathic pain vary and include such conditions as failed back surgery syndrome (FBSS), complex regional pain syndrome (CRPS), central post-stroke pain, phantom limb pain, peripheral and central nerve system injury, and post-spinal cord injury pain (Dworkin et al., 2003). Chronic neuropathic pain is most common in the back and legs.

Shealy et al. (1967) were the first to report that electrical stimulation of the dorsal spinal cord relieves cancer pain. Spinal cord stimulation (SCS) has since been applied not only to numerous cases of intractable pain but also to other conditions such as angina pectoris (AP), ischemic pain, and persistent vegetative state (Morita et al., 2007; Börjesson et al., 2008; Pedrini and Magnoni, 2007). Taylor (2006) reported that SCS not only reduces the pain but also improves quality of life in patients with FBSS or CRPS. He also reported that SCS is a cost-saving therapy. Kumar et al. (2007) reported that SCS provides better pain relief than conventional medical management alone in FBSS patients, and this was supported by a multicenter trial (Manca et al., 2008). Furthermore, the European Federation of Neurological Society guidelines support the effect of SCS in patients with FBSS or CRPS (Cruccu et al., 2007). For the central pain (spinal cord or brain lesions), SCS was reported to have some effect for pain relief. Katayama et al. (2001) reported that 7% of post-stroke pain patients revealed pain reduction with SCS and Kumar et al. (2006) also reported that SCS relieved 79% of the chronic pain due to multiple sclerosis. Thus, SCS is an essential treatment for relief of chronic neuropathic pain.

Oakley and Prager (2002) investigated some of the mechanisms underlying relief of pain by SCS. SCS was shown to stimulate the neurons of the dorsal horn of the spinal cord to release increased amount of acetylcholine and GABA and decreased amounts of aspartate and glutamate in rat models (Meyerson and Linderoth,

* Corresponding author. Department of Neurosurgery, Osaka University Faculty of Medicine, 2-2 Yamadaoka, Suita, 565-0871, Japan.
E-mail address: neurosaitoh@mbk.nifty.com (Y. Saitoh).

1053-8119/$ – see front matter © 2009 Elsevier Inc. All rights reserved.
doi:10.1016/j.neuroimage.2009.10.054

2000; Schechtmann et al., 2008). SCS was also shown to induce neurophysiological change, normalizing neuronal hyperexcitability in the dorsal horn (Yakhnitsa et al., 1999). In addition to these spinal mechanisms, functional alteration at the supraspinal level has been suggested to play an important role in pain reduction. Physiological study revealed cortical modulation during SCS (Polácek et al., 2007; Schlaier et al., 2007). However, the mechanism of pain relief by SCS is not fully understood. Brain activation during SCS has been analyzed by means of $H_2{}^{15}O$ positron emission tomography (PET) in patients with AP (Hautvast et al., 1997) and by means of functional magnetic resonance imaging (fMRI) in patients with FBSS (Kiriakopoulos et al., 1997; Stancák et al., 2008).

The investigators reported that SCS activates the primary and secondary sensorimotor cortex, cingulate cortex, insula, thalamus, and premotor cortex. Pain relief continues for several hours after SCS, so most patients with chronic pain use SCS intermittently, for example, several times per day. The modulation of brain activity after SCS has not been thoroughly examined.

In the present study, we used $H_2{}^{15}O$ PET to investigate the pattern of SCS-related neuronal activation and/or attenuation before and after SCS. $H_2{}^{15}O$ PET visualizes regional cerebral blood flow (rCBF), which reflects focal neuronal activation (Kapur et al., 1994). We also used statistical parametric mapping of normalized brain images to identify functionally specialized brain responses.

Materials and methods

Patients and surgical procedure

Nine patients (six men and three women) with intractable neuropathic pain in their lower extremities were included in this study (Table 1). Patients ranged in age from 28 to 65 years. The intractable neuropathic pain was due to FBSS in three patients, CRPS in two, cerebral hemorrhage in two, spinal cord infarction in one, and spinal cord injury in one. Pain was left-sided in five patients, right-sided in two patients, and bilateral in two patients. One of two patients with bilateral pain (patient 3) had more severe pain in right leg and the other (patient 8) had more severe pain in left leg. Their purposes of SCS were to reduce the pain in the more painful leg. Medical therapy had not been satisfactory, and the nine patients suffered from the intractable pain for 31 to 147 months before SCS was tried. Five of the nine patients showed slight to moderate motor weakness, and all had slight to severe sensory disturbance in the affected legs (Table 1). A visual analog scale (VAS), ranging from 0 to 100, and the short form of the McGill Pain Questionnaire (SF-MPQ) were used to evaluate the degree of pain.

The standard surgical procedure was used to place the SCS lead. In brief, under local anesthesia, a quadripolar electrode lead (Pisces Quad, 3487A; Medtronic, Inc., Minneapolis, MN, USA) was inserted percutaneously into the epidural space of the lumbar or thoracic spine by fluoroscopic guidance. The electrode was finally positioned after electrical sensation was detected in the region of pain upon stimulation. After confirmation of pain reduction in response to stimulation for 5–10 days, the electrode was connected to a subcutaneously implanted stimulator (Itrel III; Medtronic, Inc.).

Habitual bipolar stimulation was used for pain relief, and stimulation parameters varied between patients. General stimulation parameters were as follows: voltage, max 10 V; frequency, 10–85 Hz; pulse width, 210 to 450 μs; and duration of stimulation, 30 min. The patients controlled the stimulation at will and used SCS for at least 6 months before the PET study.

PET scanning procedure and activation task

The PET study was performed 6 to 12 months after implantation of the stimulation electrode. A Headtome-V PET scanner (Shimadzu, Kyoto, Japan) was used to scan in the three-dimensional acquisition mode with a shield to protect against scattered rays. Patients went without spinal cord stimulation for more than 12 h before the PET study. The patients lay with eyes closed in a silent and dim room. A 15-min transmission scan was acquired first with ^{68}Ge sources to correct for γ-ray attenuation. Relative CBF was measured based on the distribution of radioactivity after a slow bolus i.v. injection of $H_2{}^{15}O$ (7 mCi/scan, each lasting 90 s). Six PET scans corresponding to six $H_2{}^{15}O$ injections were obtained before SCS, SCS was performed for 30 min under the habitual condition, and six PET scans were obtained after pain reduction was confirmed. The PET protocol was the same as the motor cortex stimulation (MCS) protocol described previously (Kishima et al., 2007).

Data analysis

Attenuation-corrected data were reconstructed into an image (voxel sizes, $2\times2\times3.125$ mm; field of view, $256\times256\times196$ mm) with a resulting resolution of $4\times4\times5$ mm at FWHM (full width at half maximum). The images were analyzed with statistical parametric mapping (SPM) software (SPM2; Wellcome Department of Cognitive Neurology, London, UK) (Friston et al., 1991). PET images were anatomically normalized to fit with ICBM coordinates of the Montreal Neurological Institute. Images from each patient were realigned to the first volume of PET images and normalized to the template (Friston et al., 1995a) to account for variation in gyral anatomy and inter-individual variability in the structure–function relation and to improve the signal-to-noise ratio. This procedure was used for image realignment, anatomic normalization, smoothing (12 mm at FWHM), and statistical analysis (Kiebel et al., 1997). Data were normalized to global blood flow (average = 50). State-dependent differences in global blood flow were subjected to ANCOVA.

All nine patients were included in the same statistical analyses, with voxel-to-voxel comparison. Statistical parametric maps (SPM) were generated with an ANOVA model with the General Linear Model formulation of SPM2 (Friston et al., 1995b). We analyzed the main effect of SCS by comparing images obtained after SCS with those

Table 1
General characteristics of patients with deafferentation pain.

Patient	Age (years), sex	Etiology of pain	Pain laterality	Motor (0–5)	Sensory (0–10)	Duration of pain (months)	Pre-SCS VAS	Post-SCS VAS
1	44, M	Spinal infarction	Rt	4	4	36	80	40
2	60, F	Putaminal hemorrhage	Lt	4	10	99	100	55
3	65, F	FBSS	Bi (Rt > Lt)	5	10	147	90	30
4	45, M	CPRS	Lt	2	2	65	60	20
5	41, M	FBSS	Rt	3	5	54	85	25
6	28, F	CRPS	Lt	2	2	31	70	60
7	59, M	Putaminal hemorrhage	Lt	5	1	59	55	50
8	50, M	Spinal injury	Bi (Rt < Lt)	5	6	42	60	40
9	38, M	FBSS	Lt	5	10	57	85	45

FBSS, failed back surgery syndrome; CRPS, complex regional pain syndrome; Rt, right; Lt: left; Bi, bilateral; Motor, MMT score (0, complete paresis; 5, normal); Sensory, sensory scores (0, anesthesia; 10, normal); Pre-SCS VAS, VAS of pre-SCS; Post-SCS VAS, VAS of post-SCS.

Table 2
Increased rCBF after SCS.

Area	Cluster		Talairach coordinates (x, y, z mm)	Voxel equiv. Z
	p (corrected)	Size (voxels)		
(A) Rt thalamus	0.006	197	11.9, −15.6, 0.0	4.64
(B) Rt orbitofrontal (BA11)	0.040	161	43.6, 51.8, −12.7	4.70
(C) Lt Inf. parietal (BA7)	0.009	178	−33.7, −61.8, 45.5	4.39
(D) Rt Sup. parietal (BA7)	0.014	158	37.6, −45.9, 53.9	4.57
(E) Lt anterior cingulate (BA24)	0.001	301	−7.98, 38.1, 23.4	4.64
(F) Lt dorsolateral prefrontal (BA10)	0.050	100	−33.7, 36.0, 18.4	4.27

Rt, right; Lt, left; Inf, inferior; Sup, superior.

obtained before SCS, with the statistical threshold set at $p<0.02$ (corrected for multiple comparisons) in False Discovery Rate (FDW) for peak height, corrected for spatial extent (>8 voxels per cluster), and the cluster size was set at 100 contiguous voxels.

This method was used to generate SPM (t) of rCBF changes associated with each comparison. For between-group comparisons, the SPM (t) maps were transformed into SPM (z), and the levels of significance of areas of activation were assessed according to the peak height of foci estimation based on the theory of random Gaussian fields.

Three patients had been treated to reduce the right lower limb pain (patients 1, 3, and 5). MRIcro (http://www.sph.sc.edu/comd/rorden/mricro.html) was used to invert the images obtained from these patients from the right to the left so that statistical analysis would be consistent with that of other patients. The images were then realigned, normalized, and analyzed as previously described. Furthermore, to detect the correlation of the rCBF change and SCS efficacy, these images were performed covariance analysis with the VAS reduction rate after SCS ((pre-VAS − post-VAS) / pre-VAS).

Significance was accepted if a cluster showed a cluster corrected threshold of $p<0.05$. Anatomical locations were indicated according to the atlas of Talairach and Tournoux (1988).

This study adhered to the guidelines of the Declaration of Helsinki on the use of human subjects in research, and the patients provided written informed consent. This study was approved by the ethics committee of Osaka University Hospital.

Results

Pain reduction after SCS

After SCS, all nine patients showed various degrees of pain reduction according to VAS data (76.1 ± 25.2 to 40.6 ± 4.5) (Table 1). The pain reduction began during SCS and continued for at least 120 min after SCS. The degree of pain reduction remained stable for 60 min during the post-SCS PET scanning phase. In general, results of the SF-MPQ were for the most part compatible with VAS scores.

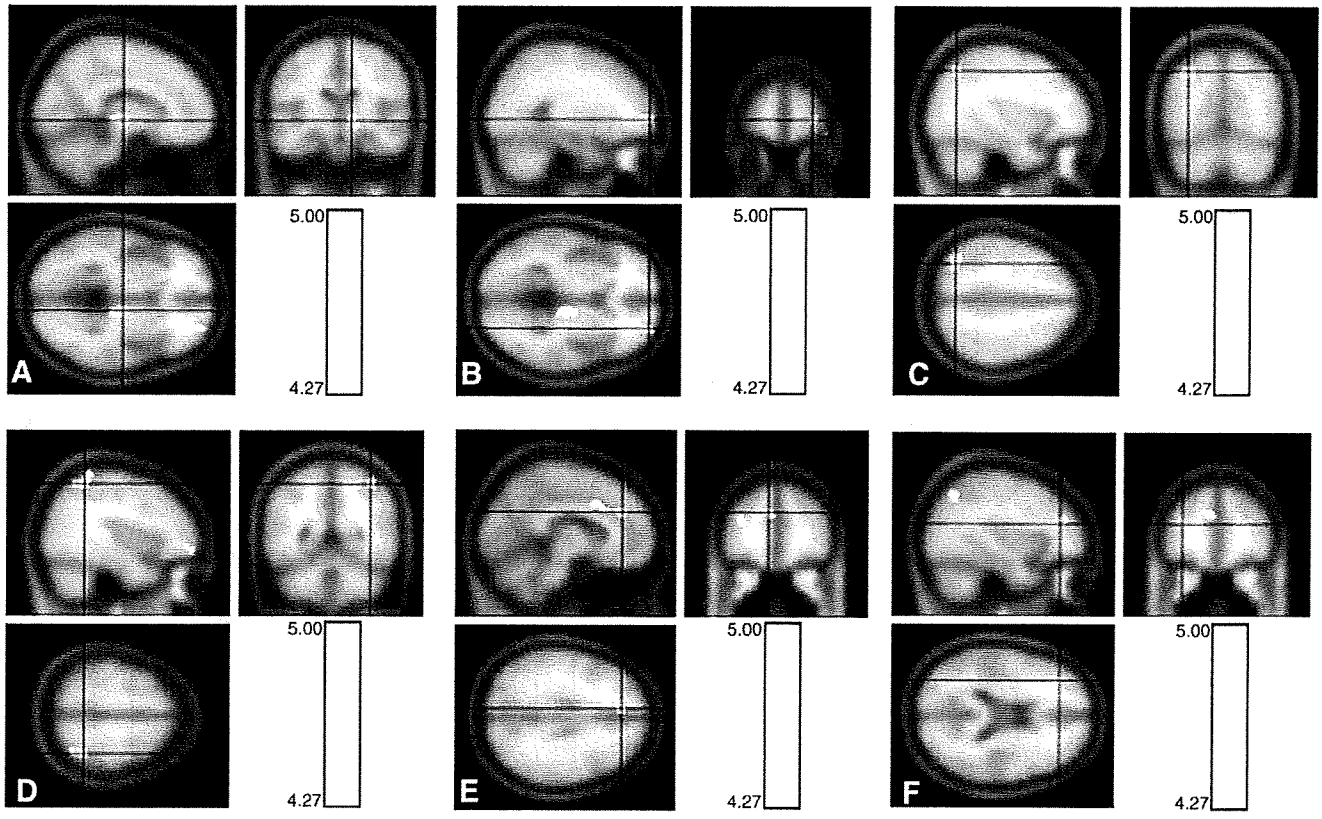

Fig. 1. Statistical parametric maps (Z maps) of intensity in normalized images. Comparison of rCBF before and after SCS shows that rCBF is increased after SCS in the right thalamus (A), right orbitofrontal cortex (BA11) (B), left inferior parietal lobule (C), right superior parietal lobule (D), left anterior cingulate cortex (E), and left dorsolateral prefrontal cortex (F). Colored bar indicates Z value (threshold, $p<0.05$). Panels A–F correspond to Table 2.